Arquivos do Museu Nacional, Rio de Janeiro, v.64, n.1, p.73-92, jan./mar.2006
ISSN 0365-4508

# GEOCHEMISTRY OF THE GLÓRIA QUARTZ-MONZODIORITE: IMPLICATIONS FOR PALEOPROTEROZOIC EVOLUTION OF THE SOUTHERN SECTOR OF THE MINEIRO BELT, MINAS GERAIS STATE, BRAZIL [1]

(With 14 figures)

CIRO ALEXANDRE ÁVILA [2]
WILSON TEIXEIRA [3]
HÉCTOR ROLANDO BARRUETO [2]
RONALDO MELLO PEREIRA [4]

ABSTRACT: The Glória quartz-monzodiorite originated at 2188 ± 29 Ma ago in the central segment of the Paleoproterozoic Mineiro belt is intrusive into the Rio das Mortes greenstone belt. Most of the major, minor and trace elements have not been extensively modified during the regional metamorphism. The Glória quartz-monzodiorite shows a calc-alkaline, metaluminous, arc-related geochemical signature, and displays major and minor trace element differences among the recognized fine, fine/medium and medium-grained facies. The medium-grained facies rocks show $SiO_2$ variation (from 58.2% to 64.3%) that allows subdivision into two sub-facies (medium I and II). The REE contents of the fine/medium and medium-grained sub-facies I show prominent LREE enrichment ($[La/Yb]_N$ between 29.7 and 38.0) and weak negative Eu anomalies. Geochemical modeling and trace element ratios support that the chemical differences resulted from progressive fractional crystallization of amphibole in fine, fine/medium and medium I sub-facies and plagioclase in medium II sub-facies. Overall field observations, geochemistry and age determinations of coeval Paleoproterozoic plutons in the region between Lavras and São João del Rei cities indicate that the Glória quartz-monzodiorite represents the old body of the pre-collisional phase of the Mineiro belt.

Key words: Glória quartz-monzodiorite. Geochemistry. Geochemical modeling. Paleoproterozoic. Mineiro belt.

RESUMO: Geoquímica do Quartzo Monzodiorito Glória: implicações para a evolução paleoproterozóica do setor sudeste do Cinturão Mineiro, Estado de Minas Gerais, Brasil.

O Quartzo Monzodiorito Glória é um corpo máfico associado à evolução paleoproterozóica do Cinturão Mineiro, porção sudeste do Cráton São Francisco, Estado de Minas Gerais, Brasil. Este é intrusivo nas rochas do *greenstone belt* Rio das Mortes e tem idade de cristalização de 2188 ± 29 Ma. Suas rochas podem ser subdivididas em fácies fina, fina/média e média, as quais apresentam assinatura geoquímica cálcio-alcalina, metaluminosa e de arco magmático. A variação do conteúdo de $SiO_2$ (de 58,2% a 64,3%) das rochas da fácies média permitiu a subdivisão da mesma em duas sub-fácies: média I e média II. O padrão de distribuição dos ETR da fácies fina/média e da sub-fácies média I apresenta pronunciado enriquecimento dos ETRL ($[La/Yb]_N$ entre 29,7 e 38,0) e sutil anomalia negativa de Eu. A caracterização geoquímica e as razões entre os elementos traços apontam que as diferenças observadas entre as fácies e sub-fácies devem-se ao fracionamento de anfibólio nas fácies fina, fina/média e sub-fácies média I e de plagioclásio na sub-fácies média II. Os dados geoquímicos, as observações de campo e os dados radiométricos de corpos plutônicos da região entre Lavras e São João del Rei apontam que o Quartzo Monzodiorito Glória é, até o presente momento, o representante mais antigo de composição diorítica gerado durante o estágio pré-colisional do Cinturão Mineiro.

Palavras-chave: Quartzo Monzodiorito Glória. Geoquímica. Modelagem geoquímica. Paleoproterozóico. Cinturão Mineiro.

[1] Submetido em 15 de dezembro de 2004. Aceito em 17 de janeiro de 2006.
Project carried out at Museu Nacional, Universidade Federal do Rio de Janeiro.
[2] Museu Nacional/UFRJ, Departamento de Geologia e Palentologia. Quinta da Boa Vista, São Cristóvão, 20940-040, Rio de Janeiro, RJ, Brasil. E-mail: avila@mn.ufrj.br.
[3] Universidade de São Paulo, Instituto de Geociências. Rua do Lago, 562, Cidade Universitária, 05508-080, São Paulo, SP, Brasil.
[4] Universidade do Estado do Rio de Janeiro, Faculdade de Geologia, Departamento de Geologia Aplicada. Rua São Francisco Xavier, 524/2019A, Maracanã, 20540-900, Rio de Janeiro, RJ, Brasil.

## INTRODUCTION

The origin of dioritic magmas remains one of the outstanding problems in petrology. Several models have been proposed for the origin of andesites (RINGWOOD, 1974; CAWTHORN, STRONG & BROWN, 1976), but it is uncertain whether such models can be applied to dioritic complexes, which in many cases are considered to be derived from calc-alkaline magmas (GULSON *et al.*, 1972; WEAVER & TARNEY, 1982). Meanwhile, different types of magma are formed in island arcs, including calc-alkaline ones - with complex spatial relationships. Moreover the melts derived from mantle and crust seems to have been generated at the same time, making understanding the magma genesis of the associated volcanic and plutonic rocks a difficult task.

The southern portion of the São Francisco Craton, between Lavras and Conselheiro Lafaiete cities (Minas Gerais State), displays a polycyclic geological evolution, which is in part associated to the framework of the Paleoproterozoic Mineiro belt. The products of this belt includes felsic and mafic plutons related with distinct phases of the tectonic evolution (ÁVILA, 2000; TEIXEIRA *et al.*, 2000; NOCE *et al.*, 2000), thereby making up the area potentially important for investigating petrogenesis and tectonics.

The geology of the studied area has been recently revised by ÁVILA (2000), TOLEDO (2002), RIBEIRO *et al.* (2003), QUÉMÉNEUR *et al.* (2003), MELLO (2003), and CHERMAN (2004). In addition, petrographic, geochemical, and geochronological studies were carried out on several pyroxenitic – gabbroic – dioritic bodies, named: Brumado diorite (ÁVILA, 1992, 2000), São Sebastião da Vitória gabbro (SILVA, 1996), Rio Grande diorite (COUTO, 2000), Brito quartz-diorite (ÁVILA, 2000; ÁVILA *et al.*, 2005b), Rosário, Martins and Ibituruna diorites (QUÉMÉNEUR, NOCE & GARCIA, 1994; QUÉMÉNEUR & NOCE, 2000), Forro peridotite-pyroxenite, Manuel Inácio pyroxenite-gabbro, Rio dos Peixes and Rio Grande gabbros (TOLEDO, 2002), Vitoriano Veloso gabbro and Dores do Campo quartz-diorite (RIBEIRO *et al.*, 2003), and Glória quartz-monzodiorite (ÁVILA, TEIXEIRA & PEREIRA, 2004; ÁVILA *et al.*, 2005a). All of these plutons are intrusive into the metavolcanic and metasedimentary rocks of Rio das Mortes and/or Nazareno greenstone belts – see figure 1.

This paper presents geochemical data of the Glória quartz-monzodiorite that indicate its genetic relationship with the pre-collisional phase of the Mineiro belt, supported by the SHRIMP U-Pb age (2188 ± 29 Ma) (ÁVILA *et al.* 2005a).

## REGIONAL GEOLOGY

The geology of the southern border of the São Francisco Craton comprises Archean and Paleoproterozoic rock units, the latter being genetically associated with the evolution of the Mineiro belt. As a summary, the country rocks consist predominantly of Archean TTG orthogneisses partially migmatized (Campo Belo, Bonfim, Passa Tempo complexes) and greenstone belt units (Rio das Velhas, Rio das Mortes and Nazareno) (Fig.1), partly covered by the Minas Supergroup and São João Del Rei, Carandaí and Andrelândia megasequences. On the other hand, the oldest terrane was intruded by mafic and felsic bodies, a part of which during the Paleoproterozoic (ÁVILA, 2000; TEIXEIRA *et al.*, 2000; NOCE *et al.*, 2000). In this regard, the mafic bodies of diorite composition represent a voluminous calc-alkaline plutonism, formed during the pre-collisional stage of the Mineiro belt.

The U-Pb and $^{207}Pb/^{206}Pb$ data in zircon available at regional scale in the central segment of the Mineiro belt indicate that the main period of magmatic activity took place between 2255 ± 6 Ma and 2101 ± 8 Ma ago (Fig.2). Therefore, the published Rb/Sr ages (2060-1860 Ma) in the Paleoproterozoic plutons are here interpreted as late isotopic resetting (Tab.1).

Recent geological mapping carried out in the central part of the Mineiro belt, between Lavras and Conselheiro Lafaiete cities has shown that volcanic mafic and ultramafic rocks, associated with the Barbacena (PIRES, RIBEIRO & BARBOSA, 1990) and to the Itumirim-Nazareno greenstone belts (TEIXEIRA, 1992) comprise two distinct tectono-stratigraphic units (ÁVILA, 2000). These units are the Rio das Mortes and Nazareno greenstone belts, respectively (ÁVILA, TEIXEIRA & PEREIRA, 2004) - herein adopted afterward.

The Rio das Mortes greenstone belt is composed predominantly of amphibolites and amphibole-bearing schists, interbedded with thick packages of gondites, queluzites, metapelites and, subordinately, metaultramafic rocks and quartzites. Contrastingly, the Nazareno sequence exhibits abundant metaultramafic rocks (komatiites, serpentinites, talc-chlorite schists) but displays scarce interlayered lenses of metapelites and quartzites, as well as local mafic

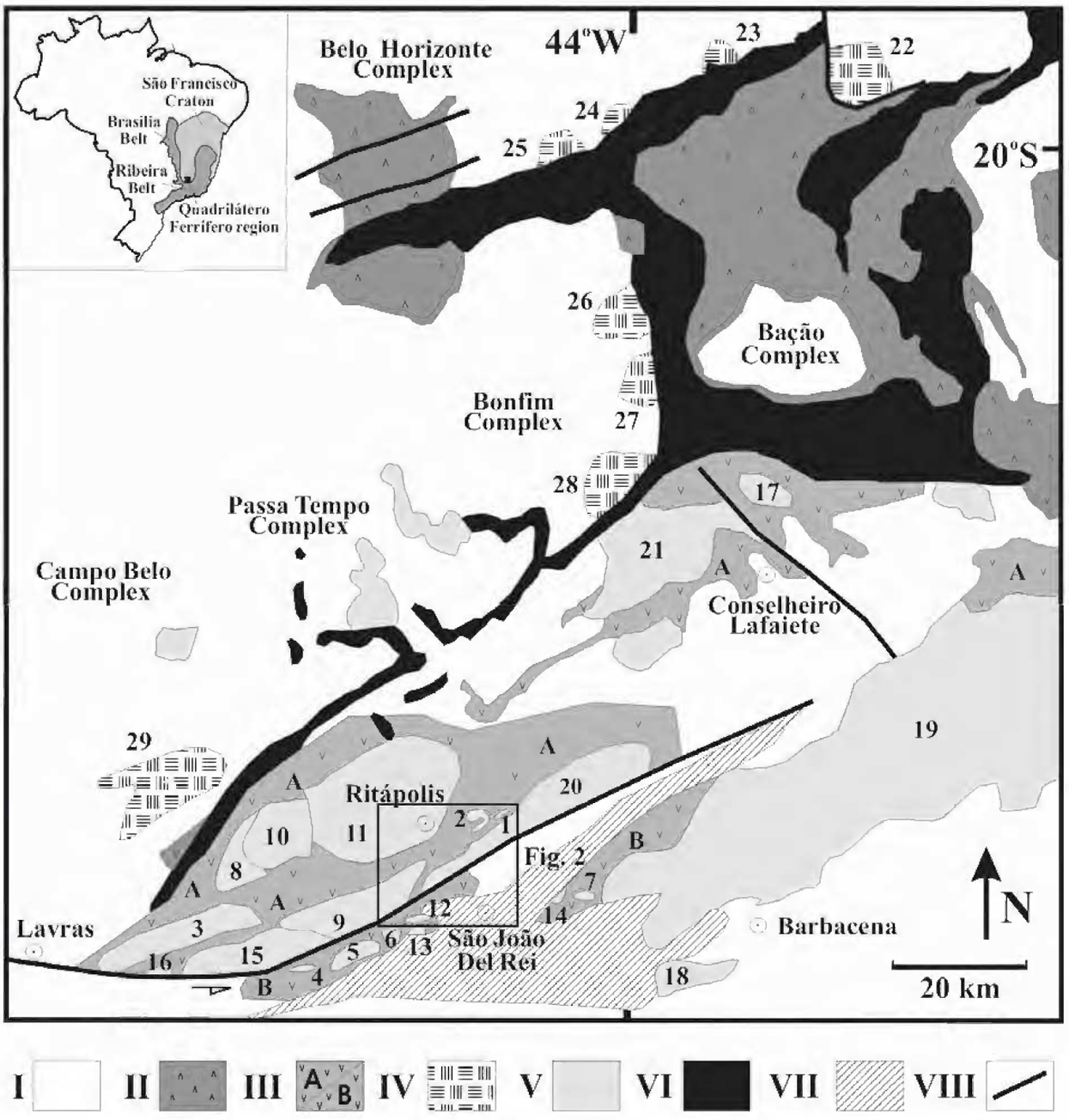


Fig.1- Archean and Paleoproterozoic plutons in the southern São Francisco Craton (adapted from ÁVILA *et al.*, 2003). I – Archean crust partly reworked during Paleoproterozoic times. II – Archean Rio das Velhas greenstone belt. III - Rio das Mortes (A) and Nazareno (B) greenstone belts. IV – Archean granitoids. V – Paleoproterozoic felsic and mafic plutons. VI – Minas Supergroup (Paleoproterozoic). VII – São João del Rei (Paleoproterozoic), Carandaí (Mesoproterozoic) and Andrelândia (Neoproterozoic) supracrustal sequences. VIII – Major structures. Keys: *Paleoproterozoic plutons*: 1 – Glória quartz-monzodiorite; 2 – Brumado diorite; 3 - Rio Grande diorite; 4 - Rio Grande gabbro; 5 - São Sebastião da Vitória gabbro; 6 – Brito quartz-diorite; 7 - Vitoriano Veloso gabbro; 8 – Ibituruna diorite; 9 – Cassiterita tonalite/trondhjemite; 10 – Tabuões trondhjemite; 11 – Ritápolis granitoid; 12 - Brumado de Baixo granodiorite; 13 - Brumado de Cima granodiorite and granophyric bodies; 14 – Tiradentes granitoid; 15 – Nazareno granite; 16 – Itumirim granitoid; 17 – Congonhas tonalite; 18 – Campolide granite; 19 – Ressaquinha complex; 20 – Fé granitic-gneiss; 21 - Alto Maranhão tonalite. *Archean plutons*: 22 – Caeté granodiorite; 23 - General Carneiro granite; 24 - Morro da Pedra granite; 25 - Ibirité granodiorite; 26 - Samambaia tonalite; 27 – Mamona granodiorite; 28 - Salto do Paraopeba granite; 29 – Bom Sucesso granite.

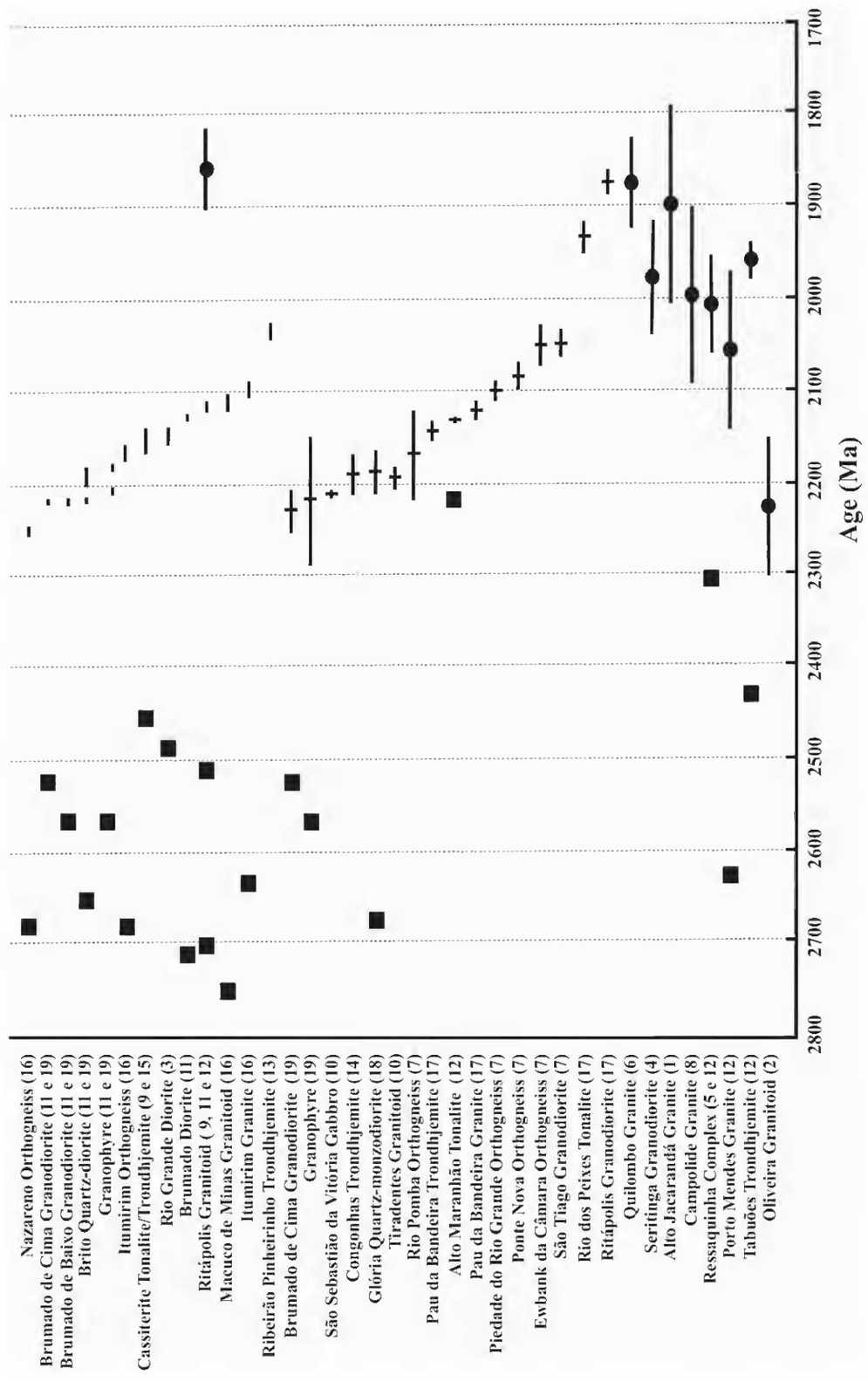


Fig.2- Crystallization age intervals of Paleoproterozoic mafic and felsic plutonic bodies in the southern border of the São Francisco Craton. Modified from ÁVILA *et al.* (2003). 1 – TEIXEIRA (1982); 2 – TEIXEIRA *et al.* (1987); 3 – CHERMAN (2002); 4 – HEILBRON *et al.* (1989); 5 – PADILHA, VASCONCELOS & GOMES (1991); 6 – CHOUDHURI *et al.* (1992); 7 – SILVA *et al.* (2002); 8 – TEIXEIRA *et al.* (2000); 9 - ÁVILA *et al.* (1998); 10 – VALENÇA *et al.* (2000); 11 – ÁVILA (2000); 12 – NOCE *et al.* (2000); 13 – EVANGELISTA, PERES & MACAMBIRA (2000); 14 - ROSA-SEIXAS *et al.* (2002); 15 – ÁVILA *et al.* (2003); 16 - CHERMAN (2004); 17 – CAMPOS (2004); 18 - ÁVILA *et al.* (2005a); 19 - ÁVILA *et al.* (2005b). Square - $T_{DM}$ age; Circle – Rb/Sr age (whole-rock isochron); full line – $^{207}Pb/^{206}Pb$ age (Pb evaporation on zircon); fill-crossed line – U-Pb zircon age (SHRIMP and isotopic dilution). Ages in millions years (Ma), except for the $T_{DM}$ ages, given in billion years (Ga). See table .

TABLE 1. Summary of the geochronological data of the plutonic bodies of the Mineiro belt.

| PLUTON | LITHOLOGY | AGE (Ma) | METHOD | $T_{DM}$ (Ma) | REF. |
|---|---|---|---|---|---|
| Nazareno orthogneiss * | Tonalite-trondhjemite | 2255 ± 6 | C | 2.68 | 13 |
| Brumado de Cima * | Granodiorite | 2239 ± 25 | A | 2.52 | 16 |
| Oliveira | Granitoid | 2228 ± 76 | D | | 2 |
| Granophyre * | Granodiorite | 2221 ± 70 | B | 2.56 | 8 e 16 |
| Brito * | Quartz-diorite | 2221 ± 2 | C | 2.64 | 8 e 16 |
| São Sebastião da Vitória * | Gabbro | 2220 ± 3 | B | | 7 |
| Brumado de Cima * | Granodiorite | 2219 ± 2 | C | 2.52 | 8 e 16 |
| Brumado de Baixo * | Granodiorite | 2218 ± 3 | C | 2.56 | 8 e 16 |
| Granophyre * | Granodiorite | 2207 ± 4 | C | 2.56 | 8 e 16 |
| Congonhas * | Trondhjemite | 2195 ± 18 | A | | 11 |
| Brito * | Quartz-diorite | 2196 ± 6 | C | 2.64 | 8 e 16 |
| Tiradentes * | Granitoid | 2194 ± 8 | B | | 7 |
| Granophyre * | Granodiorite | 2192 ± 4 | C | 2.56 | 8 e 16 |
| Glória * | Quartz-monzodiorite | 2188 ± 29 | A | 2.68 | 15 |
| Rio Pomba orthogneiss | Tonalite | 2169 ± 44 | A | | 6 |
| Itumirim orthogneiss * | Tonalite-trondhjemite | 2177 ± 4 | C | 2.68 | 13 |
| Cassiterita * | Tonalite-trondhjemite | 2162 ± 10 | C | 2.47 | 12 |
| Rio Grande * | Diorite | 2155 ± 3 | C | 2.49 | 3 |
| Brumado * | Diorite | 2131 ± 4 | C | 2.72 | 8 |
| Pau da Bandeira | Trondhjemite | 2127 ± 7 | B | | 14 |
| Alto Maranhão * | Tonalite | 2124 ± 2 | B | 2.27 | 9 |
| Ritápolis * | Granite | 2122 ± 6 | C | 2.51 | 8 |
| Ritápolis * | Granite | 2121 ± 7 | C | 2.51 | 8 |
| Pau da Bandeira | Granite | 2118 ± 7 | A | | 14 |
| Macuco de Minas | Granitoid | 2116 ± 9 | C | 2.75 | 13 |
| Piedade do Rio Grande | Tonalite | 2102 ± 8 | A | | 6 |
| Itumirim * | Granite | 2101 ± 8 | C | 2.63 | 13 |
| Ponte Nova orthogneiss | Tonalite | 2079 ± 11 | A | | 6 |
| Porto Mendes | Granite | 2061 ± 82 | D | 2.62 | 9 |
| Ewbank da Câmara | Tonalite | 2052 ± 26 | A | | 6 |
| São Tiago | Granodiorite | 2050 ± 12 | A | | 6 |
| Ribeirão Pinheirinho | Trondhjemite | 2036 ± 4 | C | | 10 |
| Ressaquinha * | Granite-tonalite | 2010 ± 52 | D | 2.30 | 9 |
| Campolide * | Granite | 1998 ± 17 | D | | 9 |
| Seritinga | Granodiorite | 1980 ± 62 | D | | 4 |
| Tabuões * | Trondhjemite | 1962 ± 20 | D | 2.43 | 9 |
| Rio dos Peixes | Tonalite | 1937 ± 22 | B | | 14 |
| Alto Jacarandá | Granite | 1900 ± 108 | D | 2.90 | 1 |
| Ritápolis * | Granodiorite | 1887 ± 19 | B | 2.71 | 14 |
| Quilombo | Granitoid | 1878 ± 50 | D | | 5 |
| Ritápolis * | Granite | 1863 ± 44 | D | 2.71 | 9 |
| Itutinga | Granite | | | 2.77 | 9 |
| Fé * | Granite | | | 2.68 | 8 |

(A) U-Pb SHRIMP (zircon); (B) U-Pb isotopic dilution (zircon); (C) $^{207}Pb/^{206}Pb$ (Pb evaporation on zircon); (D) Rb/Sr (whole rock isochron); Ref.: references. 1 - TEIXEIRA (1982); 2 - TEIXEIRA *et al.* (1987); 3 - CHERMAN (2002); 4 - HEILBRON *et al.* (1989); 5 - CHOUDHURI *et al.* (1992); 6 - SILVA *et al.* (2002); 7 - VALENÇA *et al.* (2000); 8 - ÁVILA (2000); 9 - NOCE *et al.* (2000); 10 - EVANGELISTA, PERES & MACAMBIRA (2000); 11 - ROSA SEIXAS *et al.* (2002); 12 - ÁVILA *et al.* (2003); 13 - CHERMAN (2004); 14 - CAMPOS (2004); 15 - ÁVILA *et al.* (2005a); 16 - ÁVILA *et al.* (2005b). (*) Plutons in figure 1.

flows and sills (concordant-layered amphibolites).

The studied region was affected by at least three distinct metamorphic-deformational events. The first one, of low- to medium grade amphibolite facies, affected the metaultramafic, metamafic, and metasedimentary rocks of the Nazareno and Rio das Mortes greenstone belts and give the association Mg-hornblende/Fe-hornblende + oligoclase/andesine ± chlorite ± epidote ± biotite ± sphene ± ilmenite in the metamafic rocks (TOLEDO, 2002). The second event developed under greenschist- and low- amphibolite facies, and affected regionally not only the Nazareno and Rio das Mortes greenstone belts, but also dunites, pyroxenites-gabbros and paleoproterozoic intrusions of the Mineiro belt. The metamorphic association of Paleoproterozoic diorites and gabbros is actinolite ± albite ± epidote ± biotite ± sphene (SILVA, 1996; ÁVILA, 2000). This event was coeval with deformation and folding of the greenstone belt sequences, leading to subvertical foliation (NNE-SSW strike direction) and a regional scale orientation of most plutonic and volcanic units. The third event, of greenschist facies, is associated to the Neoproterozoic tectonic events that surrounded the southern extremity of the São Francisco Craton and developed NE-SW faults and shear zones (RIBEIRO *et al.*, 1995).

## GEOLOGY OF THE GLÓRIA QUARTZ-MONZODIORITE

The Glória quartz-monzodiorite crops out between the cities of Ritápolis and Coronel Xavier Chaves, and exhibits a NNE-SSW regional foliation. It is intrusive into banded gneisses, amphibolites, schists, and metapelites of Rio das Mortes greenstone belt (Fig.3), according to the 2188 ± 29 Ma SHRIMP U-Pb zircon age (ÁVILA *et al.* 2005a).

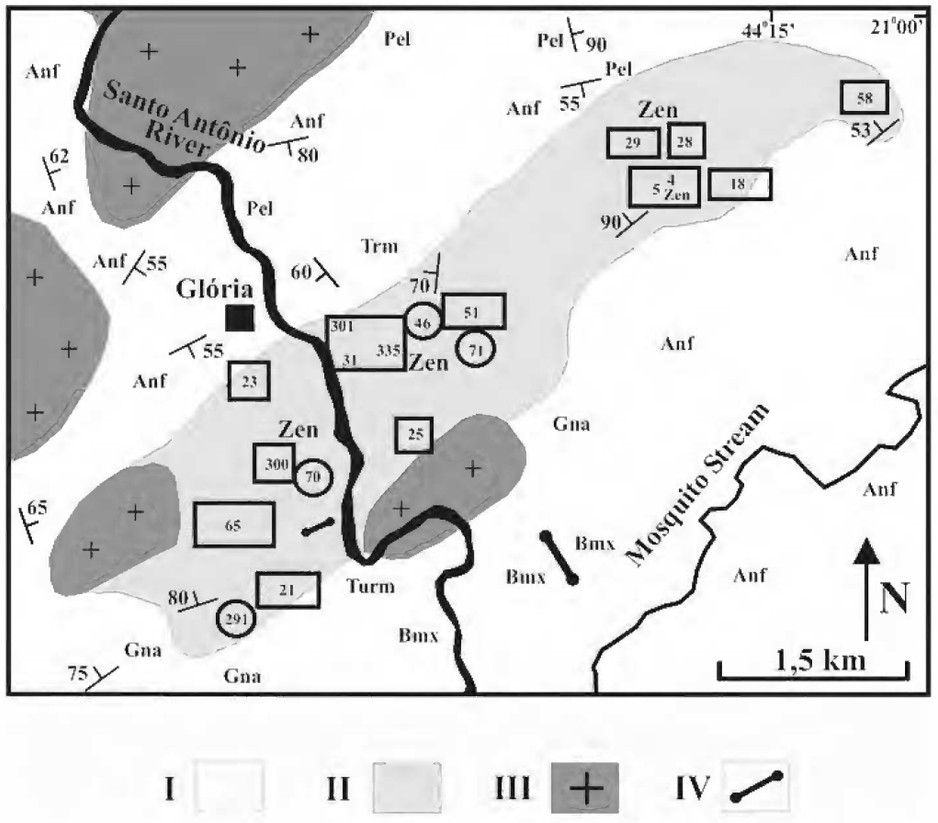


Fig.3- Geology of Glória quartz-monzodiorite and distribution of its mineral facies. Adapted from ÁVILA, TEIXEIRA & PEREIRA (2004). I - Rio das Mortes greenstone belt. II - Glória quartz-monzodiorite. III - Ritápolis granitoid. IV – Mafic dykes. (O) Fine fácies; (□) Fine/medium fácies; (▭) Medium fácies. Rocks: (Trm) tremolitite, (Anf) amphibolite, (Bmx) biotite-muscovite schist, (Gna) banded gneiss, (Pel) pelite, (Turm) turmalinite, (Zen) enclave zones.

Major minerals of the intrusion comprise calcic plagioclase, green hornblende, brown biotite, quartz, and potassic feldspar. Metamorphic phases are actinolite, albite, sphene, light brown biotite, epidote, sericite, chlorite, and carbonate. The accessory minerals are apatite, zircon, allanite, and ilmenite. Primary textures are given by equigranular hypidiomorphic crystals and, subordinately, intergranular quartz grains.

The grain-size variation (between 0.1 and 4.0 mm) reported for the Glória quartz-monzodiorite made possible its petrographic subdivision into three different facies (ÁVILA, TEIXEIRA & PEREIRA, 2004). The fine-grained facies, which is the oldest, has a restricted occurrence and is commonly cross-cut by the most widespread fine/medium-grained facies. The youngest medium-grained facies occurs mainly as apophyses and tabular injections, and displays sharp contacts with the formers. Relicts of primary minerals are observed in all the recognized facies.

In general, the modal composition of the Glória quartz-monzodiorite (quartz-diorite, quartz-monzodiorite and tonalite, with rare quartz-monzodioritic terms) is similar to those found in the Brumado (ÁVILA, 2000), Rio Grande (COUTO, 2000), and Ibitutinga diorites (QUÉMÉNEUR, NOCE & GARCIA, 1994) that occur in the vicinities. However, the Glória quartz-monzodiorite has potassic feldspar content up to 20% (Tab.2).

The mineral composition of the Glória quartz-monzodiorite is distinguished from that of the contemporary São Sebastião da Vitória (SILVA, 1996), Rio Grande and Rio dos Peixes gabbros (TOLEDO, 2002) by the lack of pyroxene and the presence of potassic feldspar. Compared to the Ritápolis, Cassiterita, Brumado de Cima, and Brumado de Baixo bodies (ÁVILA, 2000), the Glória quartz-monzodiorite has lesser quartz and potassic feldspar and higher amphibole as well as mafic minerals modal contents (Tab.2).

Quartz-feldspathic aplites, quartz- and epidote-bearing veins, granitic dykes and pegmatitic injections cross cut the Glória quartz-monzodiorite. The two latter injections are related to the Ritápolis granitoid (2121 ± 7 Ma; ÁVILA, 2000), as supported by field and petrographic relationships.

Table 2. Mineral distribution intervals of selected bodies of the Mineiro belt, southern portion of the São Francisco Craton.

| PLUTON | Qz | Plag | Biot | K-feld | Amph | Pyrx | mafic | Ref |
|---|---|---|---|---|---|---|---|---|
| Glória quartz-monzodiorite | 5.0-21.2 | 27.0-59.0 | 7.0-21.0 | 0-21.0 | 0-24.0 | 0 | 30.0-53.0 | 1 |
| Brumado diorite (medium facies) | 4.0-22.6 | 31.4-57.4 | 10.6-44.9 | 0-5.3 | 9.2-41.7 | 0 | 33.7-57.1 | 2 |
| Rio Grande diorite | Tr-24.0 | 32.0-62.0 | Tr-12.0 | 0 | 15.0-50.0 | 0 | 29.5-52.0 | 3 |
| Ibituruna diorite | 5.0-15.0 | 44.0-55.0 | 2.0-4.0 | 5.0-10.0 | 10.0-20.0 | 0 | n.d. | 4 |
| São Sebastião da Vitória gabbro | 0-2 | 48.4-61.8 | 0 | 0 | 0.2-17.2 | 28.4-45.4 | 39.2-51.6 | 5 |
| Brumado de Baixo granodiorite | 31.0-47.1 | 33.9-42.0 | Tr-4.6 | 15.7-23.0 | 0 | 0 | 2.3-9.2 | 2 |
| Brumado de Cima granodiorite | 25.4-37.5 | 32.7-48.6 | Tr-9.4 | 12.8-22.6 | 0-Tr | 0 | 4.4-11.9 | 2 |
| Cassiterita tonalite/trondhjemite | 23.2-43.9 | 43.2-69.4 | 3.3-12.0 | 0-7.8 | Tr-1.2 | 0 | 5.1-14.0 | 2 |
| Brito quartz-diorite | 8.0-13.0 | 65.0-82.0 | 3.0-15.0 | 0-3.0 | 0 | 0 | 5.0-19.0 | 2 |
| Ritápolis granitoid | 25.0-45.0 | 30.0-63.0 | Tr-16.0 | 0-40.0 | 0 | 0 | 1.0-17.0 | 2 |

(Qz) quartz; (Plag) plagioclase; (Biot) biotite; (K-feld) potassic feldspar; (Amph) amphibole; (Pyrx) pyroxene; (Epid) epidote; (Op.M) opaque minerals; (Sph) sphene; (Apat) apatite; (Zr) zircon; (Allan) allanite; (Chlor) chlorite; (% maf.) mafic minerals percent. Ref: 1 - ÁVILA, TEIXEIRA & PEREIRA (2004); 2 - ÁVILA (2000); 3 - COUTO (2000); 4 - QUÉMÉNEUR, NOCE & GARCIA (1994); 5 - SILVA (1996).

Mineralogical transformations of the Glória primary assemblage were attributed to at least two different sub-solidus events (metamorphism and potassic metasomatism). The metamorphic event caused orientation of amphibole, development of sodic plagioclase, epidote and sphene, and forming crystal aligned parallel to the regional structural trend. This implies that the intrusion crystallized before crustal shortening of the Mineiro belt. The metasomatic minerals occur only at contact with granitic dykes related to the Ritápolis granitoid, during which amphibole in the Glória mineral assemblage was partially or completely replaced by biotite and/or chlorite.

## METHODOLOGY

The analyzed samples were selected after petrography characterization. The chemical analyses of eleven samples were carried out in the laboratories of Lake-field Geosol and X-ray fluorescence of the Universidade Federal do Rio de Janeiro, Rio de Janeiro, Brazil. Data from the two laboratories are similar within the error. The analytical routines of the former laboratory comprise: X-ray spectrometry (Philips PW2400) for the analysis of the major and minor elements ($SiO_2$, $TiO_2$, $Al_2O_3$, $FeO_{Tot}$, MnO, MgO, CaO, $K_2O$, $P_2O_5$) as well as $Cr_2O_3$ and NiO; atomic absorption spectrometry, after dissolution with HF + $HClO_4$ for $Na_2O$; decomposition with HF + $H_2SO_4$ in platinum crucible buffered for FeO with $CO_2$ evolution and FeO titullation with $KMnO_4$; electrode of specific ion in alkaline fusion for F; loss of ignition by calcination at 1000°C under constant weight; X-ray fluorescence spectrometry using pressed powder pellets, for Cl, S, Th, Ba, Nb, Cs, U, Rb, Hf, Sr, Y and Zr, and plasma spectrometry (ICP) of pre-concentrated in resin of ion exchange for the Rare Earth Elements (REE).

In the Universidade Federal do Rio de Janeiro, the major elements ($SiO_2$, $TiO_2$, $Al_2O_3$, $Fe_2O_{3Tot}$, MnO, MgO, CaO, $K_2O$, $Na_2O$ and $P_2O_5$) were analyzed by X-ray fluorescence spectrometry (Phillips PW2400 with Rh-bearing tube) on samples fused with Li-tetraborate. Loss of ignition was obtained by heating rock powder at 950°C up to steady weight. Trace elements (Cr, Ni, V, Co, Zn, Rb, Ba, Sr, Nb, Ga, Y e Zr) were analyzed by X-ray fluorescence spectrometry, using one gram of powder pressed pellets.

## WHOLE ROCK GEOCHEMISTRY – RESULTS AND DISCUSSION

Chemical data for the major and trace elements, excluding the REE, are presented in table 3. The Glória quartz-monzodiorite presents significant variations of major, minor, and trace element contents. The fine/medium facies samples have restrict variation of $SiO_2$ (from 57.20% to 58.81%), whereas one sample of the fine facies group presented $SiO_2$, MgO, CaO, and $Na_2O$ contents compatible with the typical range of the fine/medium facies group. The medium facies samples show large variation of $SiO_2$ contents (from 58.20% to 64.30%), which allowed its separation into two distinct sub-facies: medium I and medium II. Samples of medium I sub-facies have a narrow $SiO_2$ contents (58.20% to 59.22%), whereas samples of medium II sub-facies displays a wider range of $SiO_2$, $Al_2O_3$, MgO, and CaO contents, when compared to the fine and fine/medium facies samples (Tab.3). Modal compositions of the analysed samples are shown in figure 4.

The Harker's diagrams display distinct evolution trends, with positive correlations for $Al_2O_3$ and $Na_2O$ with $SiO_2$ of the fine and fine/medium facies and medium I sub-facies samples and negative correlations for the same oxides of medium II sub-facies. The peculiar behavior of the medium II sub-facies is also corroborated by the negative correlation trends displayed for $TiO_2$, CaO, and $P_2O_5$ with $SiO_2$ and positive trend displayed for $K_2O$ (Fig.5).

The relationships among the major elements indicate that the studied samples are metaluminous (Fig.6), with sub-alkaline nature (Fig.7) and medium-K calc-alkaline filiation (Figs.8-9). However, samples PC-18B, CT-335A and BC-05N show contrasting high modal proportion of microcline and biotite, and thus higher $K_2O$ content. These samples fit the typical evolved high-K calc-alkaline rocks.

The limited chemical variation observed among the fine, fine/medium, and medium I sub-facies samples in the Harker diagrams supports a common evolution under similar conditions. In addition, the presence of relicts of igneous phase and/or igneous textures in the fine/medium facies, medium I and medium II sub-facies co-existing with metamorphic mineral associations, suggest that these samples underwent metamorphic conditions from greenschist- to low- amphibolite facies (see preview section). Therefore, this precludes no substantial exchanges of major, minor, and trace elements. In contrast, the metasomatic episode (see above)

resulted in significant petrography changes in the Glória samples. However, the observed mineral changes appear to be restricted to contacts with the dyke apophysis related to the Ritápolis granitoid.

The scattered patterns displayed by Rb, Ba, Sr, Zr, and Y with $SiO_2$ (Fig.10) do not agree with the strong Sr positive correlation observed in the fine and fine/medium facies and medium I sub-facies, as well as with negative correlations observed for the medium II sub-facies one. The positive correlations of Sr with $SiO_2$ displayed by the samples of the fine, fine/medium, and medium I sub-facies clearly contrasts with the negative correlation of Sr and CaO with $SiO_2$ shown by the medium II sub-facies samples (Fig.11a). All these features are consistent with the idea that plagioclase doesn't played a significant role during fractionation of the fine and fine/medium facies and medium I sub-facies.

The increase of plagioclase modal percent in the fine and fine/medium facies and medium I sub-facies, from 37% to 59% (Fig.11b) accompanies $Al_2O_3$ increase (from 14.02% to 15.07%), whilst CaO (5.82% and 6.16%) variation is restrict. Similarly, Sr content increases with the proportions of plagioclase for almost constant CaO (Fig.11a), whereas the negative correlation of MgO with $SiO_2$ accompanies decreasing of biotite and amphibole modal contents (Fig. 11c). This pattern points out the role of broad participation of amphibole during the formation of the fine and fine/medium facies and medium I sub-facies.

The fine/medium facies and medium I sub-facies are characterized by enrichment of the LREE ($[La/Yb]_N$ between 29.7 and 38.0) and slight negative Eu anomalies (Fig.12; Tab.4). On the light of these data, the high concentrations of the LREE can be attributed either to the fractionation of allanite and/or to crustal contamination.

TABLE 3. Chemical results (wt %) of major, minor and trace elements for the samples of the different facies of Glória quartz-monzodiorite.

| Rock | PC-18B | CT-335A | BC-04A1 | BC-05N | BC-04C | CT-300 | BC-05G1 | BC-05G | PC-18A | PC-18E | PC-18E1 |
|---|---|---|---|---|---|---|---|---|---|---|---|
| Classification | QD | QMd | QMd | QMd | QD | QD | QD | QD | QD | QD | QD |
| Facies | ○ | ♦ | ♦ | ♦ | ● | ● | ● | ● | △ | △ | △ |
| $SiO_2$ | 57.5 | 57.2 | 58.81 | 57.78 | 58.64 | 58.2 | 59.14 | 59.22 | 64.3 | 60.9 | 59.4 |
| $TiO_2$ | 1.1 | 0.83 | 0.82 | 0.88 | 0.82 | 1.1 | 0.89 | 0.83 | 0.66 | 0.73 | 0.75 |
| $Al_2O_3$ | 13.6 | 14.2 | 14.72 | 14.37 | 14.67 | 14.6 | 15.07 | 14.57 | 14.6 | 15.9 | 16.6 |
| $Fe_2O_{3(t)}$ | 7.08 | 7.3 | 6.58 | 6.83 | 6.59 | 8.41 | 6.34 | 6.35 | 5.65 | 6.21 | 6.29 |
| MnO | 0.13 | 0.1 | 0.1 | 0.11 | 0.1 | 0.1 | 0.1 | 0.11 | 0.09 | 0.11 | 0.12 |
| MgO | 5.5 | 6.4 | 4.77 | 5.48 | 4.84 | 5.0 | 4.04 | 5.29 | 3.0 | 3.4 | 3.2 |
| CaO | 6.0 | 6.0 | 5.96 | 6.16 | 5.82 | 5.9 | 5.98 | 5.95 | 4.2 | 4.8 | 5.3 |
| $Na_2O$ | 3.4 | 3.5 | 4.65 | 4.05 | 4.79 | 3.2 | 5.26 | 4.73 | 3.8 | 4.5 | 5.0 |
| $K_2O$ | 3.3 | 2.7 | 2.23 | 2.63 | 2.17 | 1.8 | 1.74 | 1.87 | 2.3 | 2.1 | 1.8 |
| $P_2O_5$ | 0.79 | 0.47 | 0.46 | 0.43 | 0.47 | 0.36 | 0.41 | 0.46 | 0.27 | 0.33 | 0.33 |
| P.F. | 1.59 | 1.2 | 0.33 | 0.68 | 0.64 | 1.8 | 0.7 | 0.67 | 1.31 | 1.32 | 1.42 |
| TOTAL | 99.54 | 99.4 | 99.43 | 99.4 | 99.55 | 99.86 | 99.67 | 100.05 | 99.83 | 99.93 | 99.82 |
| Cr | 205 | 225 | 197 | 262 | 131 | 300 | 137 | 233 | 137 | 137 | 68 |
| Ni | 157 | 65 | 117 | 159 | 77 | 115 | 77 | 162 | 79 | 79 | 79 |
| Ba | 2186 | 1040 | 1254 | 1106 | 919 | 1360 | 875 | 1137 | 1059 | 1365 | 888 |
| Sr | 834 | 518 | 1206 | 978 | 1342 | 813 | 1302 | 1429 | 674 | 987 | 1240 |
| Rb | 109 | 55 | 55 | 95 | 70 | 79 | 100 | 115 | 81 | 89 | 86 |
| Nb | --- | 5 | 9 | 10 | 11 | 5 | 10 | 9 | 34 | 86 | 35 |
| Zr | 446 | 180 | 317 | 306 | 365 | 189 | 325 | 373 | 215 | 232 | 221 |
| Y | 25 | 19 | 24 | 29 | 26 | 25 | 28 | 30 | 16 | 26 | 25 |

(QD) quartz-diorite; (QMd) quartz-monzodiorite; (○) fine facies; (♦) fine/medium facies; (●) medium I sub-facies; (△) medium II sub-facies.

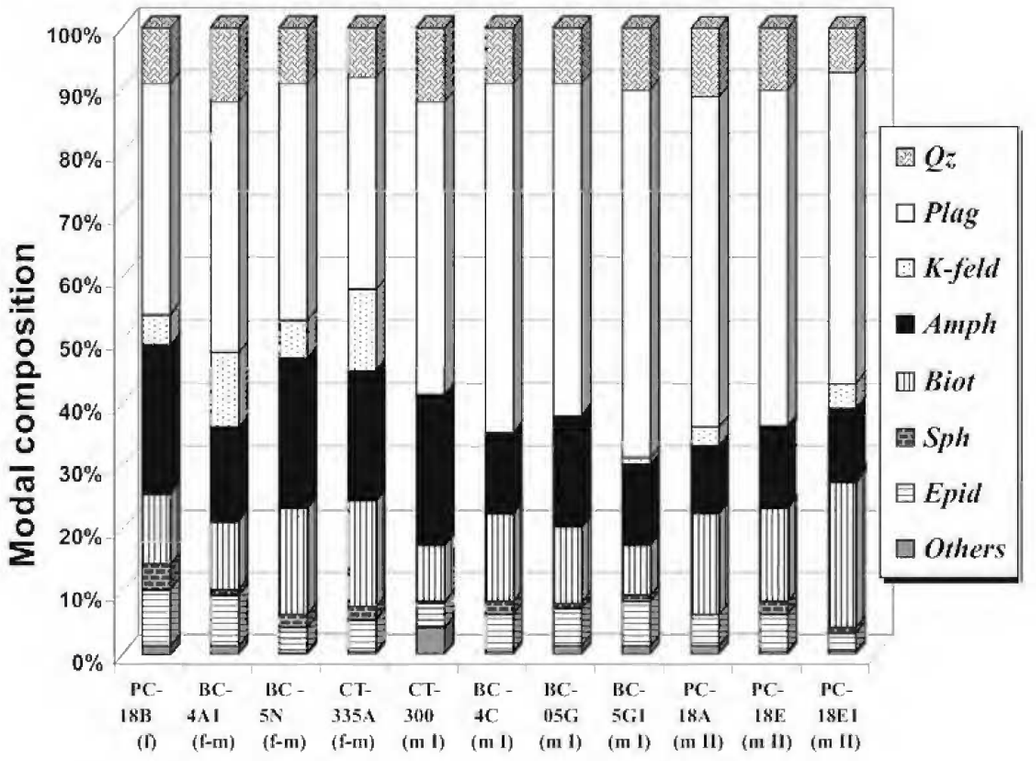


Fig.4- Bar diagram representing the modal composition (based on ÁVILA, TEIXEIRA & PEREIRA, 2004 data) for the samples of the different facies of the Glória quartz-monzodiorite. (m-I) – medium I sub-facies; (m-II) – medium II sub-facies; (f-m) – fine/medium facies; (f) – fine facies. (Qz) quartz; (Plag) plagioclase; (K-feld): potassic feldspar; (Amph) amphibole; (Biot) biotite; (Sph) sphene; (Epid) epidote; others includes: chlorite, zircon, apatite, opaque minerals, allanite, white mica and carbonate.

Table 4. Chemical analyses (ppm) of rare earth elements for the samples of the different facies of Glória quartz-monzodiorite.

| ROCK | CT-335A | CT-300 |
|---|---|---|
| CLASSIFICATION | QMd | QD |
| Facies | ♦ | ● |
| La | 84.9 | 92.9 |
| Ce | 179.9 | 121.9 |
| Nd | 87.93 | 65.16 |
| Sm | 14.43 | 9.45 |
| Eu | 2.99 | 1.97 |
| Gd | 8.13 | 5.58 |
| Dy | 5.8 | 4.11 |
| Ho | 1.1 | 0.81 |
| Er | 2.63 | 2.14 |
| Yb | 1.93 | 1.65 |
| Lu | 0.24 | 0.22 |

(QD) quartz-diorite; (QMd) quartz-monzodiorite. (♦) fine/medium facies; (●) medium I sub-facies.

The different behavior displayed by the medium II sub-facies is dependent on the plagioclase fractionation, since it controls the $Al_2O_3$, CaO, $Na_2O$, and Sr contents. The limited variation of the MgO content (between 3.0% and 3.4%) reveals the absence of any significant differentiation process involving fractionation of amphibole and biotite. This agrees well with the closely modal concentration of the sum of both minerals (25% to 27%).

The HFSE (Zr, P, Nb, and Ti) and LILE (Ba and K) signature of the fine and fine/medium facies and medium I and II sub-facies is shown in figure 13. This is consistent with the typical geochemical pattern of volcanic arc-derived rocks, as given by the Nb and Ti negative anomalies and the low Y contents. Such features would result from the retention of opaque minerals (and also garnet) in the source region. All the facies show positive Zr anomalies and occasional small negative P peaks which suggest volcanic arc-derived rocks.

The overall geochemical characteristics of the trace

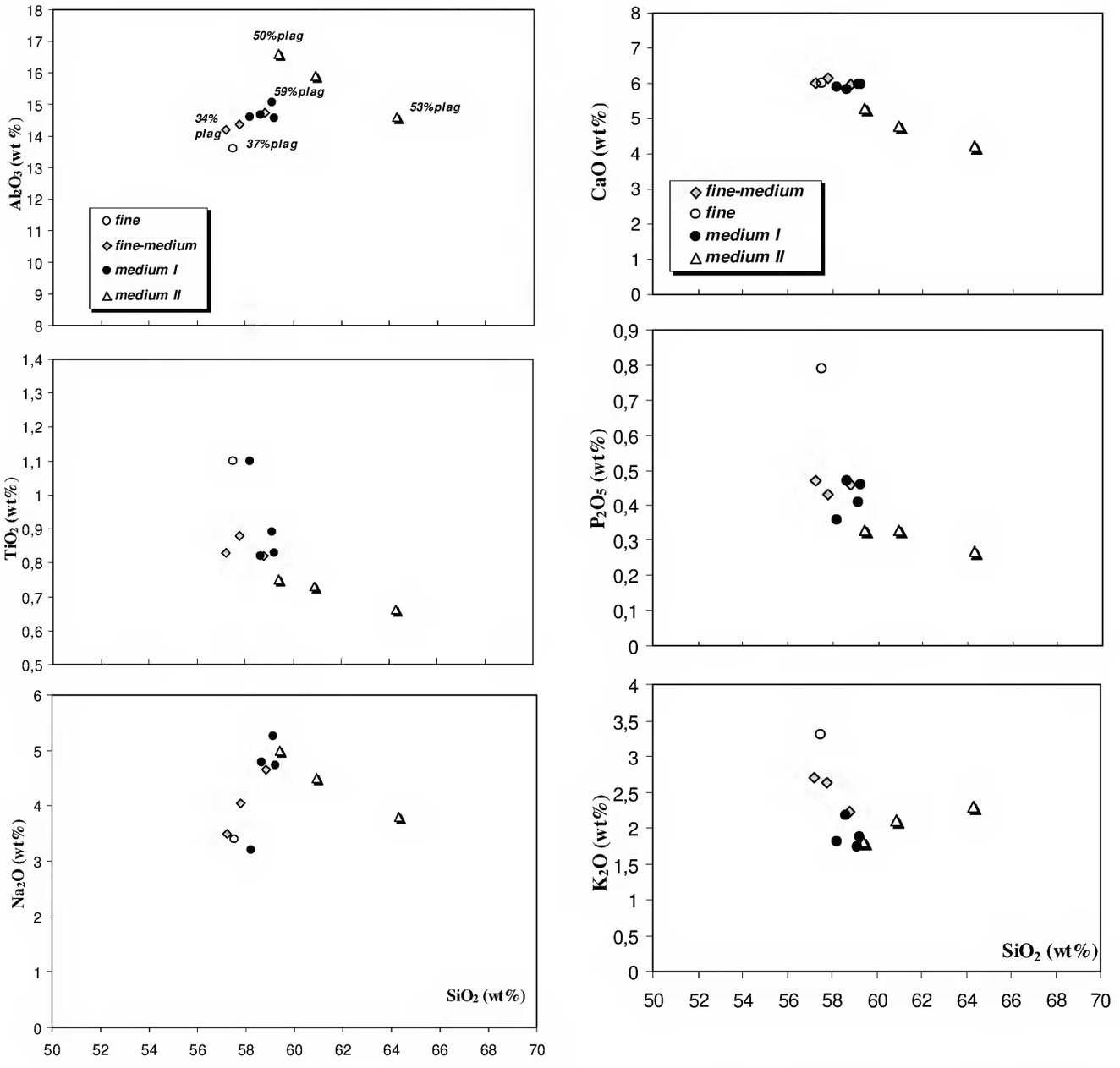


Fig.5- Harker diagrams (major elements) for the samples of the different facies of the Glória quartz-monzodiorite. (○) fine facies; (◆) fine/medium facies; (●) medium I sub-facies; (△) medium II sub-facies.

elements are consistent with magmatic evolution under low to medium pressure conditions. This conclusion is supported by: *i*) simultaneous depletion of Sr and HFSE; *ii)* P high concentrations; *iii)* variations of Ba/P ratios (0.47 to 0.87), K/Rb (135 to 407), Ba/Sr (0,67 to 2,62); *iv*) random variation of Ti/P vs. K/Rb ratios; and *v*) negative correlation of Ba/Rb vs. Rb ratios (see Tab.5).

Furthermore, the relations between Rb x (Y+Nb) are coherent with a volcanic arc environment signature (Fig. 14), as also suggested by the high Zr, Pb, Ba and K (see above). These geochemical features are comparable to that of contemporary pre-collisional intrusions of the Mineiro belt (e.g. Brumado diorite: 2131 ± 4 Ma – ÁVILA, 2000; and Cassiterita Trondhjemite/Tonalite: 2162 ± 10 Ma – ÁVILA *et al.*, 2003).

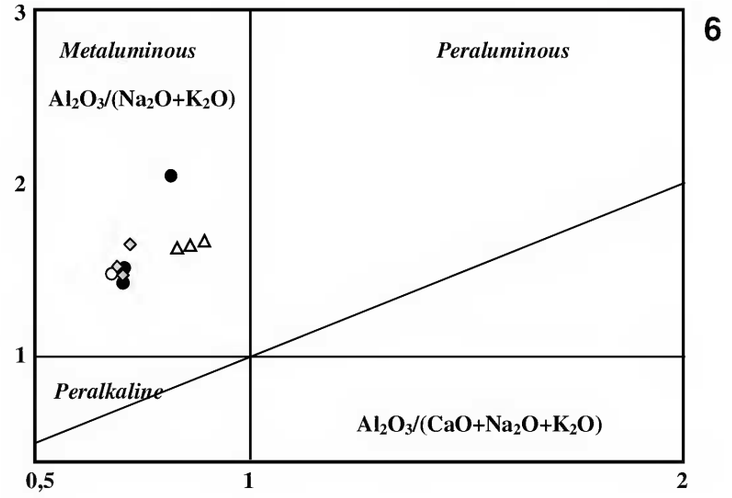


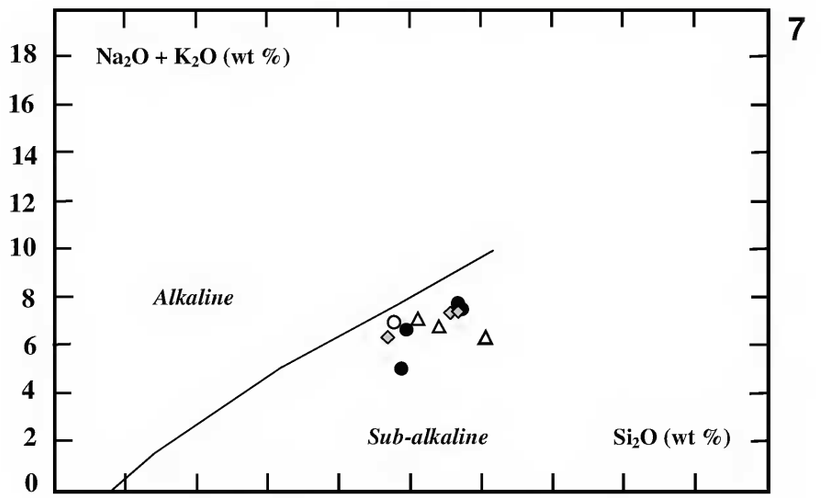


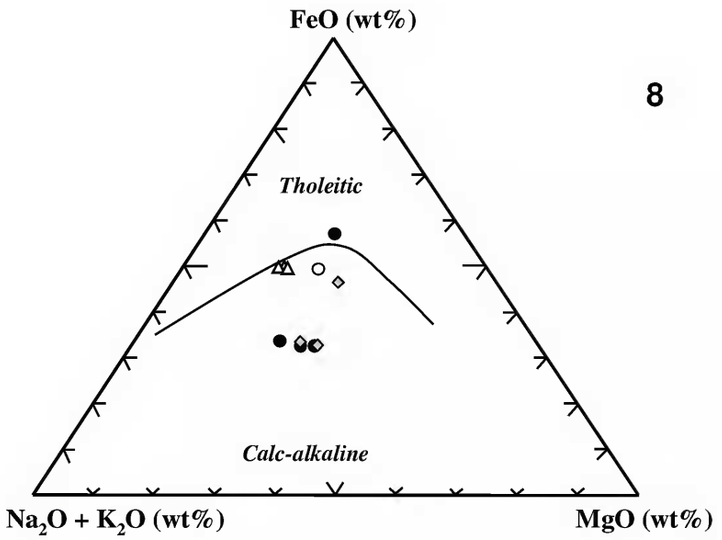


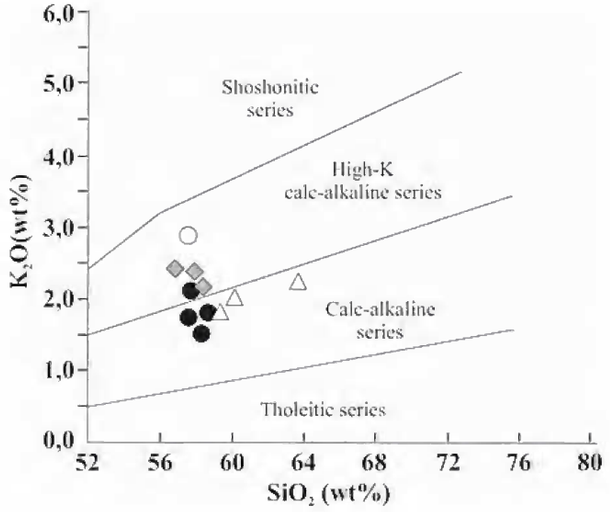


Figs.6-9- Discriminant diagrams for the samples of the different facies of the Glória quartz-monzodiorite. Fig.6- $[Al_2O_3/ (CaO + Na_2O + K_2O)]_{mol}$ x $[Al_2O_3/(Na_2O + K_2O)]_{mol}$ (MANIAR & PICOLLI, 1989). Fig.7- $SiO_2$ x $Na_2O + K_2O$ (IRVINE & BARAGAR, 1971). Fig.8- MgO-FeO*-$Na_2O + K_2O$ (IRVINE & BARAGAR, 1971). Fig.9- $SiO_2$ x $Na_2O + K_2O$ (PECCERILLO & TAYLOR, 1976). (○) fine facies; (◆) fine/medium facies; (●) medium I sub-facies; (△) medium II sub-facies.

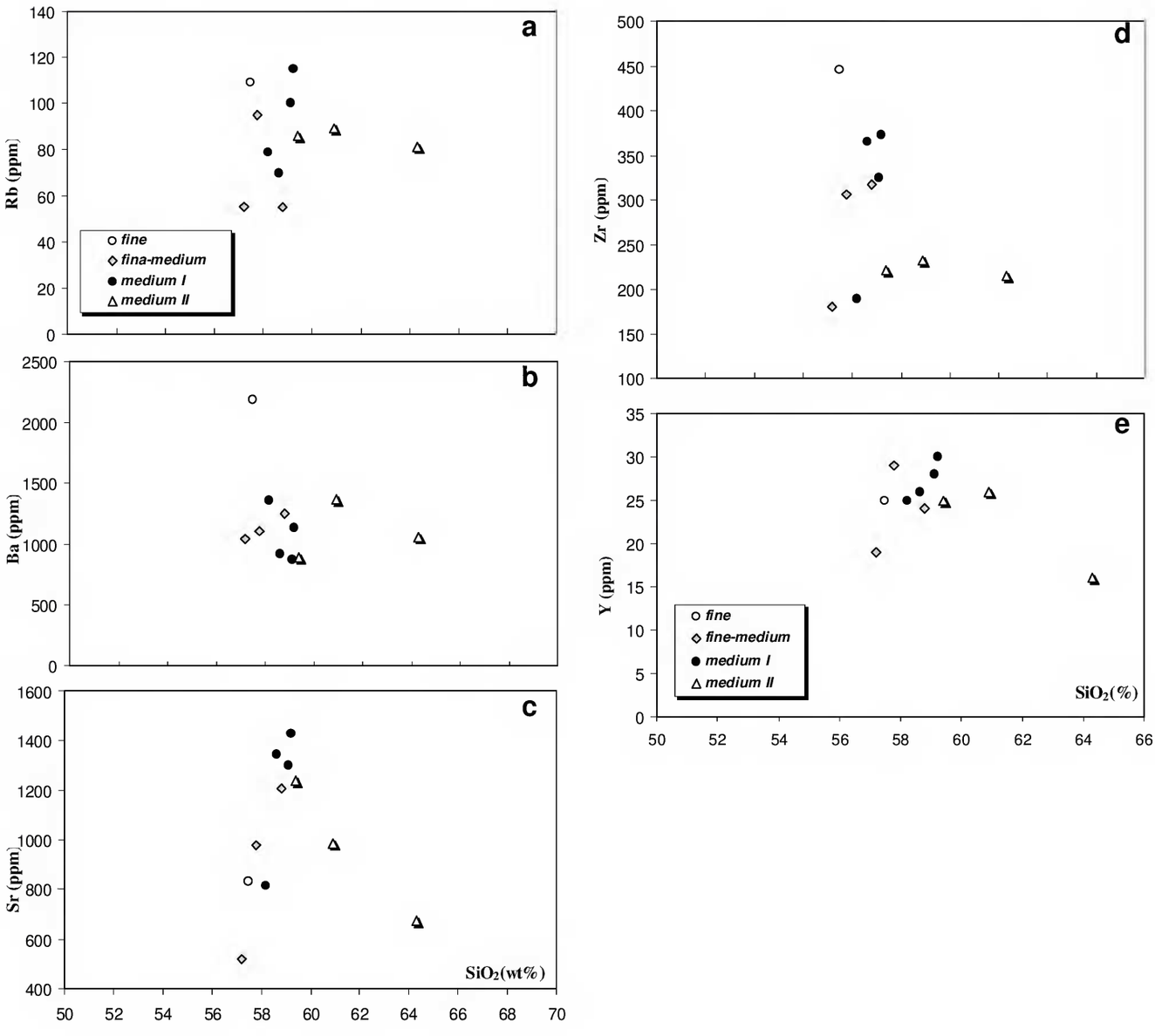


Fig.10- Harker diagrams for trace elements for the samples of the different facies of the Glória quartz-monzodiorite. (○) fine facies; (♦) fine/medium facies; (●) medium I sub-facies; (△) medium II sub-facies.

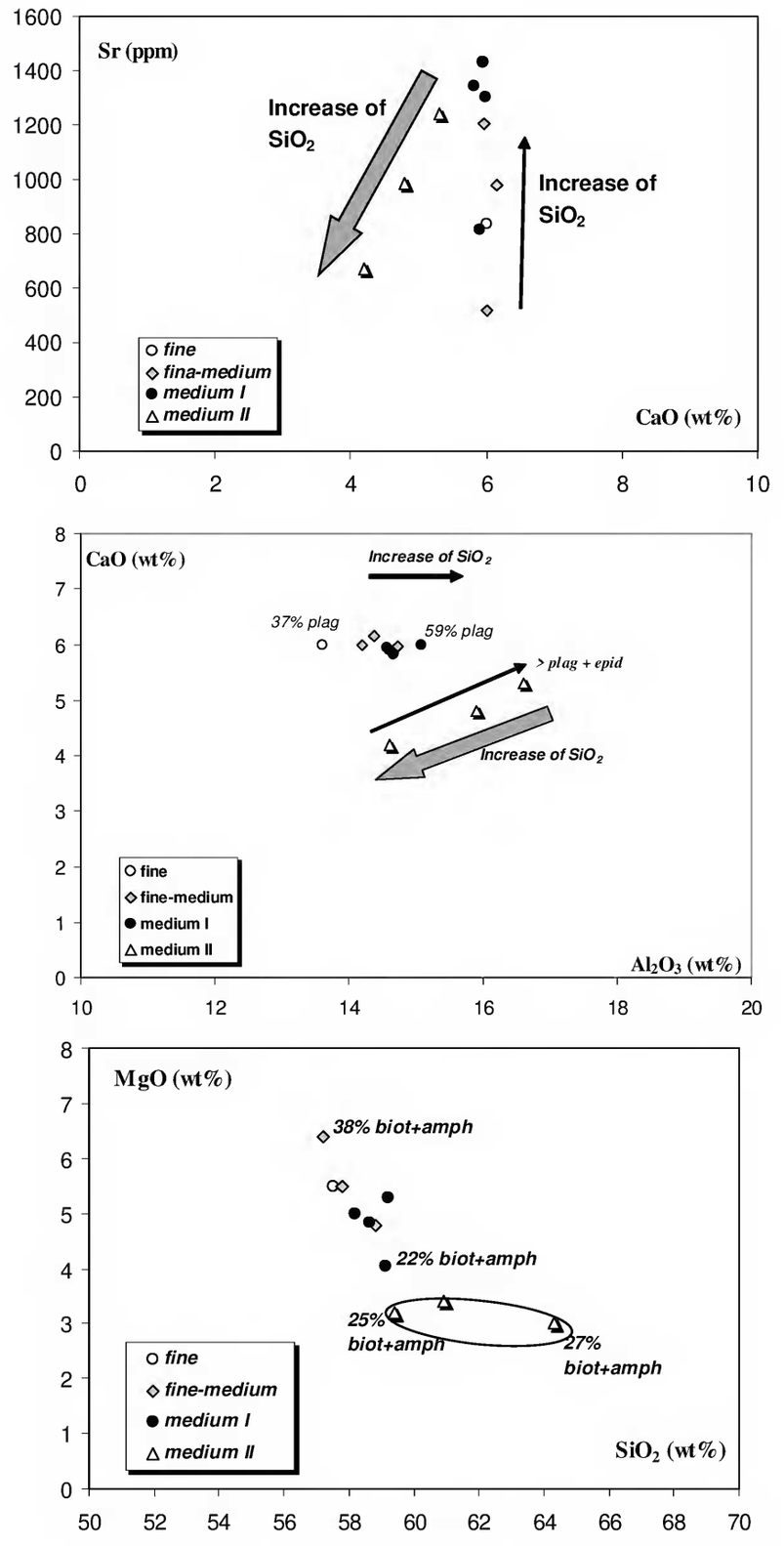


Fig.11- Diagram for the samples of the different facies of the Glória quartz-monzodiorite. (a) CaO x Sr; (b) $Al_2O_3$ x CaO; (c) $SiO_2$ x MgO. (○) fine facies; (♦) fine/medium facies; (●) medium I sub-facies; (△) medium II sub-facies.

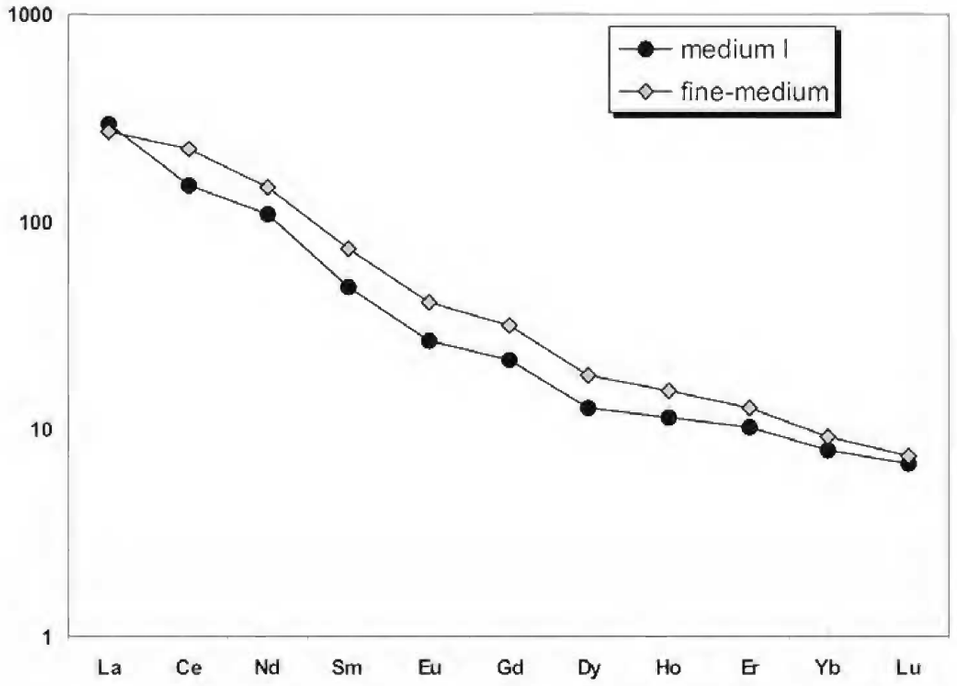


Fig.12- Distribution of the rare earth elements normalized to chondrite pattern of BOYNTON (1984). (♦) fine/medium facies; (●) medium I sub-facies.

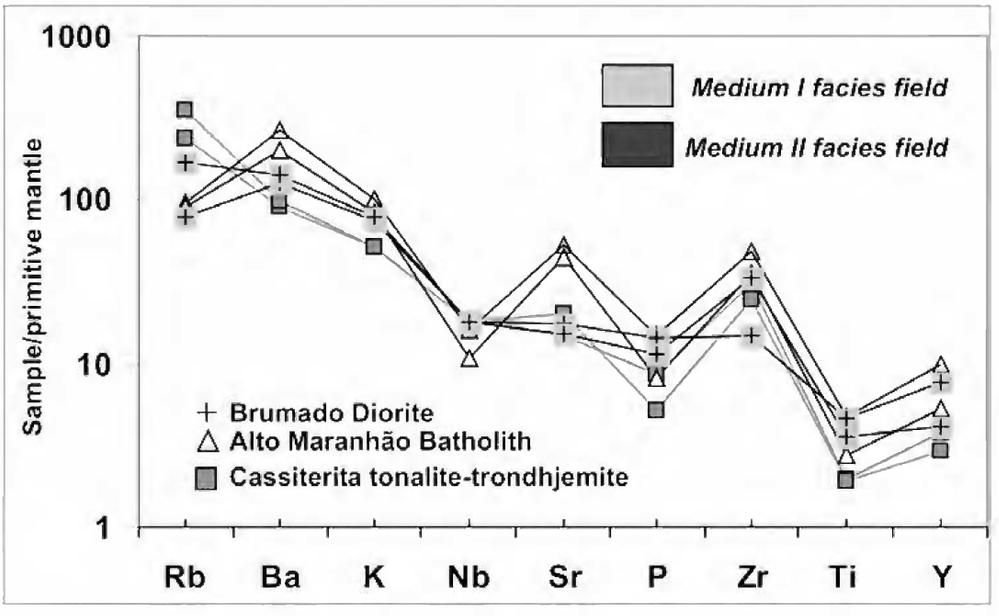


Fig.13- Spidergram of samples of medium I sub-facies and medium II sub-facies of the Glória quartz-monzodiorite. Values normalized to primitive mantle (TAYLOR & McLENNAN, 1985).

TABLE 5. Trace element ratios for the different facies samples of Glória quartz-monzodiorite.

| Rock | PC-18B | CT-335A | BC-04A1 | BC-05N | BC-04C | CT-300 | BC-05G1 | BC-05G | PC-18A | PC-18E | PC-18E1 |
|---|---|---|---|---|---|---|---|---|---|---|---|
| Classification | QD | QMd | QMd | QMd | QD | QD | QD | QD | QD | QD | QD |
| Facies | ○ | ◆ | ◆ | ◆ | ● | ● | ● | ● | Δ | Δ | Δ |
| $SiO_2$ | 57,5 | 57,2 | 58,81 | 57,78 | 58,64 | 58,2 | 59,14 | 59,22 | 64,3 | 60,9 | 59,4 |
| Zr/Y | 17,84 | 9,47 | 13,21 | 10,55 | 14,04 | 7,56 | 11,61 | 12,43 | 13,44 | 8,92 | 8,84 |
| Ba/Sr | 2,62 | 2,01 | 1,04 | 1,13 | 0,68 | 1,67 | 0,67 | 0,80 | 1,57 | 1,38 | 0,72 |
| Sr/Y | 33,36 | 27,26 | 50,25 | 33,72 | 51,62 | 32,52 | 46,50 | 47,63 | 42,13 | 37,96 | 49,60 |
| Ti/P | 1,91 | 2,43 | 2,45 | 2,81 | 2,40 | 4,20 | 2,98 | 2,48 | 3,36 | 3,04 | 3,12 |
| K/Rb | 251,33 | 407,54 | 336,59 | 229,82 | 257,35 | 189,15 | 144,45 | 134,99 | 235,73 | 195,88 | 173,76 |
| Ba/Rb | 20,06 | 18,91 | 22,80 | 11,64 | 13,13 | 17,22 | 8,75 | 9,89 | 13,07 | 15,34 | 10,33 |
| Ba/P | 0,63 | 0,51 | 0,62 | 0,59 | 0,45 | 0,87 | 0,49 | 0,57 | 0,90 | 0,95 | 0,62 |

(QD) quartz-diorite; (QMd) quartz-monzodiorite. (○) fine facies; (◆) fine/medium facies; (●) medium I sub-facies; (Δ) medium II sub-facies.

## TECTONIC IMPLICATIONS AND GEOCHEMICAL EVOLUTION

The evolution of the Mineiro belt is chiefly related to an extensive calc-alkaline plutonism, driven by complex mixture of mantle- and crustal derived end-members (ÁVILA, 2000; NOCE *et al.*, 2000; TEIXEIRA *et al.*, 2005). Particularly, the evolution of the dioritic magmatism in the Mineiro belt started with the Glória quartz-monzodiorite intrusion (2188 ± 29 Ma; ÁVILA *et al.*, 2005a) and continued with the less differentiated bodies (low K-feldspar proportions) of Rio Grande (2155 ± 3 Ma; CHERMAN, 2002), Brumado (2131 ± 4 Ma; ÁVILA, 2000), and Ibitutinga diorites.

In the Glória quartz-monzodiorite, the fine facies, fine/medium, and medium I sub-facies evolved by a combination of the fractionation of amphibole, whereas the medium II sub-facies displays different geochemical trends, here interpreted as the result of plagioclase fractionation, inasmuch as biotite and amphibole contents were well stabilized.

Moreover, the geochemical data indicate that the recognized facies (fine, fine/medium, medium I sub-facies, and medium II sub-facies) are probably co-genetic, evolved under low to medium pressure conditions (in volcanic arc - related setting), and originated at 2188 ± 29 Ma ago (SHRIMP U-Pb zircon age). The studied samples derived from a Paleoproterozoic juvenile magma slightly enriched in crustal components, as also supported by the negative $\varepsilon_{Nd(T)}$ signature (-3.4) and $T_{DM}$ model age (2.68 Ga) (ÁVILA *et al.*, 2005a).

The youngest Paleoproterozoic sin-tectonic intrusions found between Lavras and São João del Rei are pegmatites and granitic apophyses, which are ascribed to the late-magmatic activity of Ritápolis granitoid (2121 ± 7 Ma), Macucu de Minas granitoid (2116 ± 9 Ma), and Itumirim granite (2101 ± 8 Ma), respectively (ÁVILA, 2000; CHERMAN, 2004). In the São João Del Rei region, the Ritápolis granitoid caused replacement of metamorphic actinolite by metassomatic biotite along the margins of the Glória quartz-monzodiorite and Brumado diorite.

From the above geologic framework and according to the petrographic and geochemical characteristics, the Glória quartz-monzodiorite (2188 ± 29 Ma) can be related to the pre-collisional tectonic phase of the Mineiro belt. On-going isotopic and geochemical studies on adjacent Paleoproterozoic plutons will bring new insights on tectonic and magmatic aspects of the central part of the Mineiro belt.

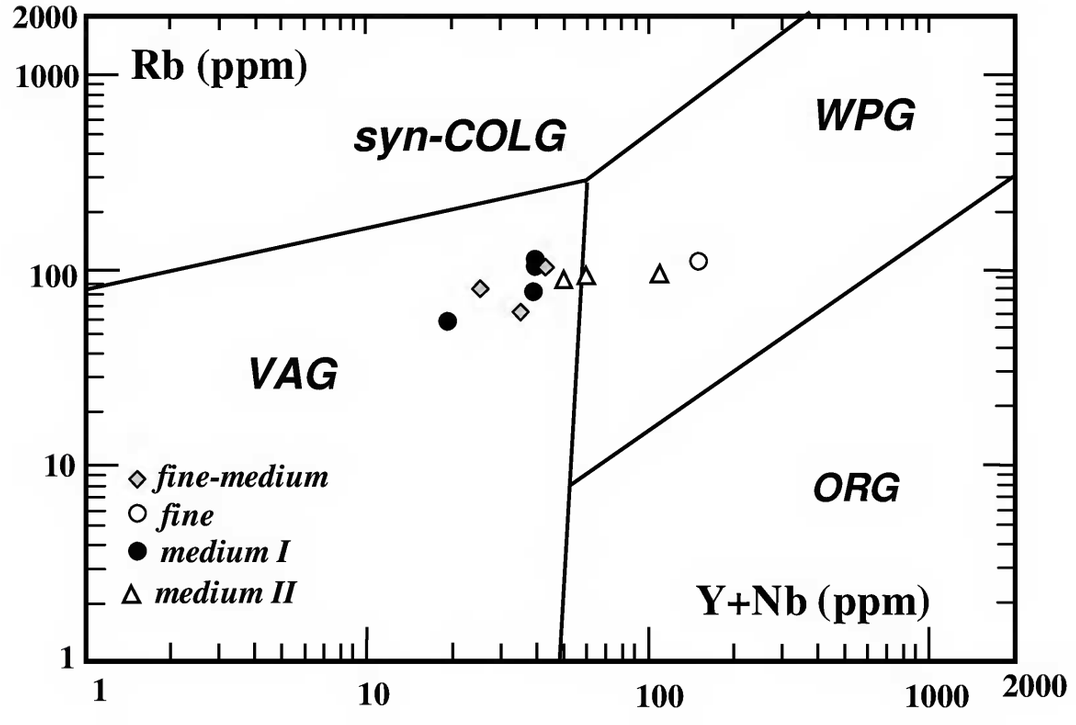


Fig.14- Rb x (Y + Nb) tectonic discrimination diagram (PEARCE, HARRIS & TINDLE, 1984) for the samples of the different facies of the Glória quartz-monzodiorite. (○) fine facies; (♦) fine/medium facies; (●) medium I sub-facies; (△) medium II sub-facies.

ACKNOWLEDGEMENTS

The authors thank Paulo Roberto Dal Cere for his participation in the preliminary studies of the Glória pluton, and Joel Gomes Valença, André Ribeiro and Rudolph Allard Johannes Trouw (Universidade Federal do Rio de Janeiro), for their support during field work. We are grateful to Elson Paiva de Oliveira (Universidade Estadual de Campinas), for critically reading the manuscript and to the anonymous reviewers whose comments greatly improved its early version. Ciro Alexandre Ávila thanks the staff of the X-ray Fluorescence Laboratory of the Universidade Federal do Rio de Janeiro, for carrying out the analyses. We acknowledge the Fundação de Amparo à Pesquisa do Estado do Rio de Janeiro (FAPERJ), for financial support (# 170.023/2003), and the associated research fellowship granted to Héctor Rolando Barrueto (# 152.564/2002). Wilson Teixeira and Ciro Alexandre Ávila thank the Conselho Nacional de Desenvolvimento Científico e Tecnológico (CNPq) for financial support (# 304300/03-9 and # 475673/04-2).

REFERENCES

ÁVILA, C.A., 1992. **Geologia, petrografia e geoquímica das rochas pré-cambrianas (Unidade Metadiorítica Ibitutinga e Unidade Metatrondhjemítica Caburu) intrusivas nas rochas do *Greenstone Belt* Barbacena, São João Del Rei, Minas Gerais**. Rio de Janeiro. 265p. Dissertação (Mestrado em Geologia), Programa de Pós-Graduação em Geologia, Departamento de Geologia, Universidade Federal do Rio de Janeiro.

ÁVILA, C.A., 2000. **Geologia, petrografia e geocronologia de corpos plutônicos paleoproterozóicos da borda meridional do Cráton São Francisco, região de São João Del Rei, Minas Gerais. Rio de Janeiro**. 401p. Tese (Doutorado em Geologia), Programa de Pós-Graduação em Geologia, Departamento de Geologia, Universidade Federal do Rio de Janeiro.

ÁVILA, C.A.; VALENÇA, J.G.; MOURA, C.A.V.; RIBEIRO, A. & PACIULLO, F.V., 1998. Idades $^{207}Pb/^{206}Pb$ em zircões de corpos metaplutônicos da região de São João Del Rei, borda sul do Cráton do São Francisco, Minas Gerais. In: CONGRESSO BRASILEIRO GEOLOGIA, 40.,1998, Belo Horizonte. **Boletim de Resumos...**, Belo Horizonte: Sociedade Brasileira de Geologia, p.75-78.

ÁVILA, C.A.; VALENÇA, J.G.; MOURA, C.A.V.; KLEIN, V.C. & PEREIRA, R.M., 2003. Geoquímica e idade do Trondhjemito Cassiterita, borda meridional do Cráton São Francisco, Minas Gerais. **Arquivos do Museu Nacional**, Rio de Janeiro, **61**(4):267-284.

ÁVILA, C.A.; TEIXEIRA, W. & PEREIRA, R.M., 2004. Geologia e petrografia do Quartzo Monzodiorito Glória, Cinturão Mineiro, porção sul do Cráton São Francisco, Minas Gerais. **Arquivos do Museu Nacional**, Rio de Janeiro, **62**(1):83-98.

ÁVILA, C.A.; TEIXEIRA, W.; CORDANI, H.G; BARRUETO, H.R.; PEREIRA, R.M.; MARTINS, V.T. & DUNYI, L., 2005a. Geoquímica e idade U/Pb do Quartzo Monzodiorito Glória: implicações na evolução paleoproterozóica do setor oriental do Cinturão Mineiro. In: CONGRESSO BRASILEIRO DE GEOQUÍMICA, 9., 2005, Porto de Galinhas. **Anais...,** Porto de Galinhas: Sociedade Brasileira de Geoquímica. (Published in CD ROM)

ÁVILA, C.A.; VALENÇA, J.G.; TEIXEIRA, W.; BARRUETO, H.R.; MOURA, C.A.V.; CORDANI, H.G; PEREIRA, R.M. & MARTINS, V.T., 2005b. Geocronologia U/Pb e Pb/Pb da Suíte Serrinha: implicações para a evolução paleoproterozóica da margem sul do Craton São Francisco. In: SIMPÓSIO DE VULCANISMO E AMBIENTES ASSOCIADOS, 3., 2005, Cabo Frio. **Anais...**, Cabo Frio: Sociedade Brasileira de Geologia, p.357-361.

BOYNTON, W.V., 1984. Cosmochemistry of the rare earth element: meteorite studies. In: HENDERSON, P. (Ed.). **Rare earth element geochemistry**. Amsterdam: Elsiever. p.63-114.

CAMPOS, J.C.S., 2004. **O lineamento Jeceaba – Bom Sucesso como limite dos terrenos arqueanos e paleoproterozóicos do Cráton São Francisco meridional: evidências geológicas, geoquímicas (rocha total) e geocronológica (U-Pb)**. 161p. Tese (Doutorado em Geologia), Programa de Pós-Graduação em Geologia, Departamento de Geologia, Universidade Federal de Ouro Preto.

CAWTHORN, R.G.; STRONG, D.F. & BROWN, P.A., 1976. Origin of corundum-normative intrusive and extrusive magmas. **Nature**, Hampshire, **259**(1):102-104.

CHERMAN, A.F., 2002. **Geologia, petrografia, feições estruturais e geocronologia dos corpos metagranitóides intrusivos no Greenstone Belt Barbacena, na região entre Lavras e Nazareno, Minas Gerais. Rio de Janeiro**. 60p. Exame de Qualificação (Doutorado em Geologia), Programa de Pós-Graduação em Geologia, Departamento de Geologia, Universidade Federal do Rio de Janeiro.

CHERMAN, A.F., 2004. **Geologia, petrografia e geocronologia de ortognaisses paleoproterozóicos da borda meridional do Cráton do São Francisco, na região entre Itumirim e Nazareno, Minas Gerais. Rio de Janeiro.** 259p. Tese (Doutorado em Geologia), Programa de Pós-Graduação em Geologia, Departamento de Geologia, Universidade Federal do Rio de Janeiro.

CHOUDHURI, A.; CROSTA, A.P.; SCHRANK, A.; SZABÓ, G.A.J. & IYER, S.S., 1992. The Quilombo Granite in the Archean Morro do Ferro Greenstone belt, SW Minas Gerais, and character of the transamazonian event. **Revista da Escola de Minas**, Ouro Preto, **45**(1/2):152-153.

COUTO, F.M., 2000. **Metadioritos, metaquartzo dioritos e metatonalitos (associação MDQT) e suas rochas encaixantes do Greenstone Belt Barbacena, na região de Lavras – Nazareno (sul do Estado de Minas Gerais)**. Rio de Janeiro. 75p. Dissertação (Mestrado em Geologia), Programa de Pós-Graduação em Geologia, Departamento de Geologia, Universidade Federal do Rio de Janeiro.

EVANGELISTA, H.J.; PERES, G.G. & MACAMBIRA, M.J.B., 2000. Pb/Pb single-zircon dating of Paleoproterozoic calc-alkaline/alkaline magmatism in the southeastern São Francisco Craton region, Brazil. **Revista Brasileira de Geociências**, São Paulo, **30**(1):174-176.

GULSON, B.L.; LOVERING, J.F.; TAYLOR, S.R. & WHITE, A.J.R., 1972. High-K diorites, their place in the calc-alkaline association and relationship to andesites. **Lithos**, Netherlands, **5**:269-279.

HEILBRON, M.; GONÇALVES, M.L.; TEIXEIRA, W.; TROUW, R.A.J.; PADILHA, A.V. & KAWASHITA, K., 1989. Geocronologia da região entre Lavras, São João del Rei, Lima Duarte e Caxambú (MG). **Anais da Academia Brasileira de Ciências**, Rio de Janeiro, **61**(2):177-199.

IRVINE, T.N. & BARAGAR, W.R.A., 1971. A guide to the chemical classification of common volcanic rocks. **Canadian Journal of Earth Sciences**, Ottawa, **8**(5):523-548.

MANIAR, P.D. & PICOLLI, P.M., 1989. Tectonic discrimination of granitoids. **Geological Society of America Bulletin**, Bolder, **101**(5):635-643.

MELLO, A.G., 2003. **Rochas metavulcânicas máficas e metacumuláticas máficas e ultramáficas do Greenstone Belt Barbacena e metagranitóides intrusivos, na área de Dores de Campos, sul do Estado de Minas Gerais**. 159p. Dissertação (Mestrado em Geologia), Programa de Pós-Graduação em Geologia, Departamento de Geologia, Universidade Federal do Rio de Janeiro.

NOCE, C.M.; TEIXEIRA, W.; QUÉMÉNEUR, J.J.G.; MARTINS, V.T.S. & BOLZACHINI, E., 2000. Isotopic signatures of paleoproterozoic granitoids from the southern São Francisco Craton and implications for the evolution of the Transamazonian Orogeny. **Journal of South American Earth Sciences**, Oxford, **13**(2):225-239.

PADILHA, A.V.; VASCONCELOS, R.M. & GOMES, R.A.A.D., 1991. Evolução geológica. In: **Barbacena. Folha SF.23-X-C-III, Estado do Minas Gerais**. Programa de Levantamentos Geológicos Básicos do Brasil, DNPM/CPRM, p.111-133.

# SEED SURFACE STRUCTURE IN THE GENUS *ZIERIA* SM. (RUTACEAE)

J. M. Powell and J. A. Armstrong

(Aeeepted for publieation 14.3.1980)


## ABSTRACT

*Powell, J. M. and J. A. Armstrong (National Herbarium of New South Wales, Royal Botanic Gardens, Sydney, New South Wales, Australia 2000) 1980. Seed surface structure in the genus* Zieria *Sm. (Rutaceae). Telopea 2 (1): 85–112.*—Seed surfaee structure of 119 samples representing 23 speeies of *Zieria* is examined, using the scanning electron mieroseope. Forty surfaee patterns are distinguished; thirty-eight are ridged, one is tubereulate and one eollieulate-ribbed. The ridged surfaee patterns can be elassified into three major groups and a number of subgroups on the basis of structural similarities. The taxonomie significance of the seed surface morphology is assessed by comparison with newly eireumscribed taxonomie entities reeognized on other morphologieal grounds by Armstrong. There is eonsiderable eoneurrence between the seed data and the taxonomie entities but it is not universal. It is eoneluded that seed surfaee features provide a useful basis for distinguishing species and subspeeies in only some instanees within this genus. The elose relationship indieated by general morphology within eertain groups of taxa is supported by the seed data although, in general, phylogenetie eonclusions eannot be based solely on seed surfaee strueture.


## INTRODUCTION

The genus *Zieria*, comprising some 27 speeies, is predominantly eastern Australian in distribution, extending from NE. Queensland to Tasmania and as far west as Kangaroo Island in South Australia; one species is endemic in New Caledonia. Bentham (1863) distinguished 10 species; since then a number of other taxa have been defined (Mueller 1875; Domin 1913; Maiden & Betche 1911, 1916; White 1932, 1942; Blakely 1941). The genus is being revised by Armstrong as part of a broader biosystematic study of the tribe Boronieae (Rutaceae).

Traditionally fruit and seed characters such as the fruit type (drupe, berry, capsule, samara), the number of cells in the fruit, the persistence or otherwise of the endocarp and the presence or absence of endosperm have been used in delimiting subfamilies and tribes within the Rutaceae (Bentham 1863; Engler 1931, 1964), but relatively little attention has been paid to seed surface structure.

Recent scanning electron microscope studies have provided detailed information on the surface patterns of small fruits and seeds (Heywood 1969, 1971) and have provided a firm base for the separation of closely related species in some genera e.g. *Carex* (Toivonen & Timonen 1976), *Cocculus* (Forman 1974), *Epilobium* (Seavey et al. 1977b), *Erica* (Huekerby et al. 1972), *Mentzelia* (Hill 1976) and *Scirpus* (Schuyler 1971), and for distinguishing subspecies and varieties within others, e.g. *Arenaria* (Ehlin 1968) and *Cochlearia* (Godeau 1973a, b). Seed surface patterns are considered to be significant at higher taxonomic levels (sections, tribes, etc.) in *Cordylanthus* (Chuang & Heckard 1972), *Epilobium* (Skvortsov & Rusanovitch 1974; Seavey et al. 1977a) and *Sagina* (Crow 1979), and have been used for assessing relationships in *Scirpus* (Schuyler 1971), in *Mentzelia* (Hill 1976) and in the Melastomataceae (Whiffin & Tomb 1972). Much of the data available has been reviewed by Brisson & Peterson (1976).

An initial survey of *Zieria* seeds revealed various surface patterns and indicated a detailed study would be worthwhile. The aims of the study were, firstly, to describe in detail the seed surface patterns found in *Zieria* and to elucidate inter- and intra-specific variability, and secondly, to assess the usefulness of the seed data for taxonomic purposes.

TABLE 1

Voucher details of *Zieria* specimens studied

| Sample Number | Taxon (Armstrong unpubl.) | Name used at NSW in 1975 | Collector & No. |
|---|---|---|---|
| 1 | *Zieria arboreseens* ssp. '*a*' | Z. arboreseens Sims | Blake 23715 (BRI) |
| 2 | ,, | ,, | Close NSW 2770 |
| 3 | ,, | ,, | Doney NSW 30526 |
| 4 | ,, | ,, | French MEL 61977 |
| 5 | ,, | ,, | Garden NSW 7311 |
| 6 | ,, | ,, | Jacobs 51 (MEL) |
| 7 | ,, | ,, | Maiden NSW 2773 |
| 8 | ,, | ,, | Merrall MEL 61989 |
| 9 | *Zieria* sp. nov. '*F*' | Z. sp. aff. arborescens | Armstrong 115 (NSW) |
| 10 | ,, | ,, | Armstrong 744 (NSW) |
| 11 | ,, | ,, | Rodway NSW 19748 |
| 12 | *Zieria aspalathoides* ssp. '*a*' | Z. aspalathoides A. Cunn. ex Benth. | Armstrong 999 (NSW) |
| 13 | ,, | ,, | Armstrong 1030 (NSW) |
| 14 | ,, | ,, | Biddulph 47 (BRI) |
| 15 | ,, | ,, | Clemens BRI 021762 |
| 16 | ,, | ,, | Henderson 706 (BRI) |
| 17 | ,, | ,, | Henderson 1206 (BRI) |
| 18 | ,, | ,, | Streimann 631 (CBG) |
| 19 | ,, | ,, | Streimann 633 (CBG) |
| 20 | *Z. aspalathoides* ssp. '*b*' | ,, | Boorman NSW 2725 |
| 21 | ,, | ,, | Forsyth NSW 2734 |
| 22 | ,, | ,, | Streimann 678 (CBG) |
| 23 | *Z. aspalathoides* ssp. '*c*' | ,, | Gittins 919 (BRI) |
| 24 | ,, | ,, | Henderson 1098 (BRI) |
| 25 | *Zieria* sp. nov. '*A*' | Z. aspalathoides var. obovata C.T. White | Armstrong 1025 (NSW) |
| 26 | ,, | ,, | Fitzalan MEL 62269 |
| 27 | ,, | ,, | Telford NQ 750 (CBG) |
| 28 | *Zieria* sp. nov. '*B*' | Z. aspalathoides var. nov. '1' | Costin NSW 10525 |
| 29 | *Zieria chevalieri* | Z. chevalieri Virot | McKee 5559 (NSW) |
| 30 | *Zieria fraseri* ssp. '*b*' | Z. compacta C. T. White | Armstrong 669 (NSW) |
| 31 | ,, | ,, | Jones CANB 189291 |
| 32 | ,, | ,, | McKee 455 (MEL) |
| 33 | ,, | ,, | McKee NSW 22018 |
| 34 | ,, | ,, | Pedley 1175 (BRI) |
| 35 | ,, | ,, | Streimann 575 (CBG) |
| 36 | *Zieria cytisoides* ssp. '*a*' | Z. cytisoides Sm. | Boorman NSW 2977 |
| 37 | ,, | ,, | Constable 5168 (NSW) |
| 38 | ,, | ,, | Gittins 351 (BRI) |
| 39 | ,, | ,, | Rodway NSW 19727 |
| 40 | ,, | ,, | Williamson MEL 62033 |
| 41 | *Zieria cytisoides* ssp. '*b*' | ,, | Burgess CBG 020402 |
| 42 | ,, | ,, | Phillips CBG 005925 |
| 43 | ,, | ,, | Phillips CBG 002887 |
| 44 | ,, | ,, | *Anon.* MEL 62038 |
| 45 | *Zieria furfuracea* ssp. '*a*' | Z. furfuracea R.Br. ex Benth. | Armstrong 551 (NSW) |
| 46 | ,, | ,, | Maiden NSW 2787 |
| 47 | *Zieria furfuracea* ssp. '*b*' | ,, | King s.n. (Coffs Harbour) |
| 48 | ,, | ,, | White BRI 021724 |
| 49 | ,, | ,, | *Anon.* BRI 021725 |
| 50 | *Zieria granulata* | Z. granulata (F.Muell.) C. Moore ex Benth. var. granulata | Boorman NSW 2855 |
| 51 | ,, | ,, | Camfield NSW 2851 |
| 52 | ,, | ,, | Camfield BRI 021617 |
| 53 | *Zieria* sp. nov. '*C*' | Z. granulata var. adenodonta F.Muell. | *Anon.* MEL 62068 |
| 54 | ,, | ,, | Carron MEL 62069 |
| 55 | ,, | ,, | White 11876 (BRI) |
| 56 | *Zieria involucrata* | Z. involuerata R.Br. ex Benth. | Armstrong 804 (NSW) |
| 57 | ,, | ,, | Hamilton NSW 55952 |
| 58 | *Zieria laevigata* ssp. '*a*' | Z. laevigata Sm. | Armstrong 750 (NSW) |
| 59 | ,, | ,, | Bäuerlen 126 (MEL) |